J Shoulder Elbow Surg (2019) 28, 949–958

ELSEVIER

Journal of Shoulder and Elbow Surgery

www.elsevier.com/locate/ymse

Overlay repair with a synthetic collagen scaffold improves the quality of healing in a rat rotator cuff repair model

Mark Zhu, MBChB[a,b,*], Mei Lin Tay, MSc[a], Karen Callon, BSc[a], Donna Tuari, RVN[a], Lei Zhao, PhD[a], Michael Dray, MBChB, FRACPA[c], Jie Zhang, PhD[a], Nicola Dalbeth, MBChB, FRACP, PhD[a,b], Jacob Munro, MBChB, FRACS, PhD[a,b], Simon Young, MBChB, FRACS, MD[a,d], Brendan Coleman, MBChB, FRACS[e], Dipika Patel, MBChB, FRCOphth[a,b], Jillian Cornish, PhD[a], David Musson, PhD[a]

[a]*University of Auckland, Auckland, New Zealand*
[b]*Auckland District Health Board, Auckland, New Zealand*
[c]*Waikato District Health Board, Waikato, New Zealand*
[d]*Waitemata District Health Board, Auckland, New Zealand*
[e]*Counties Manukau District Health Board, Auckland, New Zealand*

Background: Augmenting repairs with extracellular matrix–based scaffolds is a common option for rotator cuff tears. In this study, a new collagen scaffold was assessed for its efficacy in augmenting rotator cuff repair.

Methods: The collagen scaffold was assessed in vitro for cytocompatibility and retention of tenocyte phenotype using alamarBlue assays, fluorescent imaging, and real-time polymerase chain reaction. Immunogenicity was assessed in vitro by the activation of human monocytes. In vivo, by use of a modified rat rotator cuff defect model, supraspinatus tendon repairs were carried out in 40 animals. Overlay augmentation with the collagen scaffold was compared with unaugmented repairs. At 6 and 12 weeks postoperatively, the repairs were tested biomechanically to evaluate repair strength, as well as histologically to assess quality of healing.

Results: The collagen scaffold supported human tendon-derived cell growth in vitro, with cells demonstrating proliferation and appearing morphologically tenocytic over the experimental period. No immunogenic responses were provoked compared with suture material control. In vivo, augmentation with the scaffold improved the histologic scores at 12 weeks (8.4 of 15 vs 6.4 of 15, $P = .032$). However, no significant difference was detected with mechanical testing.

Conclusion: The new collagen scaffold was supportive of cell growth in vitro and generated a minimal acute inflammatory response. In vivo, we observed an improvement in the histologic appearance of the repair at 12 weeks. However, a meaningful increase in biomechanical strength was not achieved. Further modification and improvement of the scaffold are required prior to consideration for clinical use.

This study received approval from the Auckland University Animal Ethics Committee (R001705).

*Reprint requests: Mark Zhu, MBChB, University of Auckland, 85 Park Road, Grafton, Auckland 1023, New Zealand.
E-mail address: mzhu031@aucklanduni.ac.nz (M. Zhu).

https://doi.org/10.1016/j.jse.2018.11.044

Level of evidence: Basic Science Study; Biomechanics and Histology; Animal Model

Keywords: Animal model; rotator cuff; collagen; scaffold; bone-tendon healing; preclinical

Rotator cuff tears are a common cause of shoulder pain and functional deficits, affecting more than 20% of the population.[37] Surgical repair may be required to restore function and resolve pain in large tears.[11] For this reason, approximately 250,000 cuff repairs are performed annually in the United States.[19,22]

Despite their potential success, rotator cuff repairs have a high failure rate of 30%-70%.[1,2,21,23,25,28] Repair failure is associated with persistent pain and ongoing loss of function.[6,10,31,40] This mainly occurs at 1 to 24 months after surgery as a result of inadequate healing at the bone-tendon junction, leading to excessive loads and eventual failure at the suture-tendon interface.[5,18,21,24] In an effort to improve the outcome of surgery, tissue scaffolds have been used to augment the repair as interpositional or overlay patches.[2,29] It is hoped that these scaffolds can prevent repair failure by increasing the strength of the initial repair, as well as enhancing the quality of biological healing at the tendon and the bone-tendon junction.[2,21,24,28,31,34,36]

Commercially available products consist mostly of decellularized cadaveric tissue from human and animal sources.[2,14] It is unclear whether these materials can facilitate tissue incorporation and thereby improve the quality of healing.[2,26] The foreign tissue base of these scaffolds also raises concerns regarding the potential for chronic inflammatory reactions if DNA and cellular materials are not completely removed.[12,15,39] Overall, the outcomes after augmented repairs are inconsistent. Of 3 clinical randomized controlled trials, only 1 supported the use of tissue scaffolds whereas the others noted high repair failure rates with unacceptable inflammatory reactions in the scaffold groups.[4,7,17]

We have obtained a new collagen scaffold that is free of cellular fragments and DNA remnants that cause unfavorable host immunologic reactions.[15,39] We propose the use of this new collagen scaffold as an overlay augmentation for rotator cuff repairs. We aim to (1) assess the cellular responses to the scaffold in vitro and (2) determine whether the scaffold can improve the quality of healing and the strength of the repair in a rat in vivo model.

Materials and methods

Reagents and ethical approval

Dulbecco's Modified Eagle Medium: Nutrient Mixture F-12 (DMEM/F-12), penicillin-streptomycin mixture (10,000 U/mL), and fetal bovine serum (FBS) were obtained from Gibco (Thermo Fisher Scientific, Waltham, MA, USA). RPMI-1640 media were obtained from Sigma-Aldrich (St Louis, MO, USA).

Animal work was carried out with approval from the University of Auckland Animal Ethics Committee and adhered to the tenets of the Declaration of Helsinki. Primary human tenocytes were isolated under approval from the New Zealand Health and Disability Ethics Committee (Wellington, New Zealand).

Primary human tendon-derived cell culture

Primary tendon-derived cell culture has been previously described.[9] In brief, excess tissue from healthy human hamstring grafts was harvested and kept hydrated at 4°C until use. Tendon tissue was roughly cut into pieces smaller than 0.5 cm^2 and digested in 0.5 mg/mL of dispase and 0.5 mg/mL of collagenase (both from Sigma-Aldrich) in DMEM/F-12 with 10% FBS at 37°C for up to 18 hours until all extracellular matrix had been digested. The cell suspension was then passed through a cell strainer, washed, and resuspended in enzyme-free media. Cells were cultured in DMEM/F-12 with 10% FBS in 75-cm^2 flasks (Corning, Corning, NY, USA) and incubated at 37°C with 5% carbon dioxide until confluent. Cell cultures were frozen down for a period before being used for these experiments.

Scaffold preparation

The scaffold manufacturing process has been previously described.[38] Cultrex 3D bovine collagen I (Trevigen, Gaithersburg, MD, USA) underwent centrifugal ultrafiltration to achieve a density of 125 mg/mL. The collagen was then molded, neutralized, dehydrated, rehydrated, and cross linked using UV light exposure. The finished scaffold was cut into $5 \times 2 \times 1$–mm strips and used for both in vitro and in vivo experimentation.

Cell growth assays

Cells isolated from human hamstring tendons as described earlier were seeded in 24-well plates (Greiner Bio-One, Kremsmünster, Austria), at a density of 2.5×10^4 cells/well, and cultured in DMEM/F-12 with 5% FBS onto plastic or sterilized collagen scaffolds. Cell growth was measured on days 1, 3, and 7 with the addition of alamarBlue (Life Technologies [Thermo Fisher Scientific]) at 5% of the final concentration in wells (50 µL of alamarBlue in 1000 µL of media) for 4 hours at 37°C. At the end of this incubation, 200 µL of the alamarBlue conditioned medium was transferred to a 96-well plate (Greiner Bio-One) and fluorescence (excitation, 540 nm; emission, 630 nm) was read using a Synergy 2 multi-detection microplate reader (BioTek Instruments, Winooski, VT, USA). The changes in alamarBlue fluorescence are expressed as the ratio of each time point compared with day 1 readings in media alone. At the end of day 7, cells seeded in a plate parallel to the growth assays were harvested for cell pellets. The cell pellets collected were used to identify changes in gene expression levels.

Fluorescent imaging

Cells isolated from human hamstring tendons as described earlier were seeded in 6-well plates (Greiner Bio-One), at a density of 7.5×10^4 cells/well, and cultured in DMEM/F-12 with 5% FBS onto plastic, collagen-coated glass coverslips or sterilized collagen scaffolds. On days 1, 3, and 7, samples were labeled with CellTracker Green CMFDA Dye (Life Technologies) for 4 hours at 37°C before fixing with paraformaldehyde (4% in phosphate buffer). These were then treated with Triton-X 0.5% overnight and stained with DAPI (4',6-diamidino-2-phenylindole, dihydrochloride) (Thermo Fisher Scientific) for 2 hours at 4°C.[33] Fluorescent images were obtained using a Zeiss LSM 710 Inverted Confocal Microscope (Carl Zeiss, Oberkochen, Germany).

Gene expression

For analysis of gene expression, total cellular RNA was extracted from cultured cells and purified using TRIzol (Thermo Fisher Scientific) and the Direct-zol RNA MiniPrep kit (Zymo Research, Irvine, CA, USA). The quantity and purity of the RNA were measured using a NanoDrop Lite spectrophotometer (Thermo Fisher Scientific, Scoresby, VIC, Australia). Reverse transcription (500 ng of RNA used for each sample) was carried out using SuperScript III (Life Technologies), and complementary DNA was used for real-time polymerase chain reaction. Primer-probe sets were purchased as TaqMan Gene Expression Assays from Applied Biosystems (Thermo Fisher Scientific). Multiplex polymerase chain reaction was performed with FAM-labeled probes specific for the genes of interest and VIC-labeled 18S ribosomal RNA probes according to the company's instructions, using an ABI PRISM 7900HT sequence detection system (Applied Biosystems). Samples were assayed in triplicate. The relative level of messenger RNA expression was determined using the ΔΔCt calculation method, normalized to values of the nontreated cells.

Immunogenicity

A human monocytic cell line (THP-1) was used to test the immune response to the scaffolds as previously described.[33] Cells were seeded in 24-well plates at a density of 1.5×10^6 cells/well in RPMI-1640 with 10% FBS and 1-mmol/L NaP (sodium pyruvate) onto plastic or sterilized collagen scaffolds. One-millimeter segments of No. 4-0 Vicryl suture (Ethicon, Somerville, NJ, USA) were used as positive controls. Cell pellets were collected at 24 hours and 48 hours after seeding and used for gene expression analysis. This analysis is designed to detect the likelihood of an acute inflammatory reaction after implantation.

In vivo

We obtained 46 Sprague-Dawley rats, weighing more than 350 g and older than 12 weeks, for surgery. All rats were checked for general health and behavior and then randomized into 1 of 3 groups: (1) sham surgery group (approach to supraspinatus only, n = 6), (2) unaugmented control group (single-row supraspinatus repair, n = 20), and (3) intervention group (single-row repair augmented with collage scaffold, n = 20).

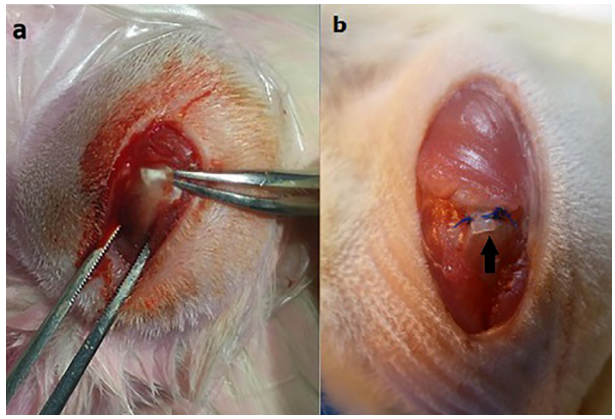

Figure 1 **(a)** Isolated supraspinatus tendon after approach. **(b)** Scaffold (*arrow*) in situ after repair.

At least 1 hour before surgery, all rats received carprofen, a nonsteroidal anti-inflammatory drug, subcutaneously (10 μL/g). Induction was performed in a sealed rodent induction box filled with 5% isoflurane. Anesthesia was maintained during surgery using isoflurane through a specially designed nose cone. A 2.5-mL subcutaneous injection of 0.9% sodium chloride was administered immediately after induction.

The left forelimb and shoulder were clipped; prepared using a 2% chlorhexidine and 70% alcohol solution; and draped using a sterile, clear drape. A 2-cm longitudinal incision was made, centered on the acromion. This allowed visualization of the supraglenoid fossa and the proximal shaft of the humerus. The belly of the deltoid was then incised in line with the muscle fibers down to bone. A small pair of blunt forceps was maneuvered around the humerus to maintain control. The proximal insertion of the deltoid was then carefully divided to allow visualization of the supraspinatus tendon (Fig. 1, *a*). To maximize the operating window, the coracoacromial arch was partially divided. A No. 5-0 Prolene stay suture (Ethicon) was placed in the supraspinatus tendon. The tendon was divided at its insertion to the greater tuberosity. The tendon footprint was then carefully débrided to remove any residual tendon tissue.

In the unaugmented group, supraspinatus repair was performed using No. 5-0 Prolene with the modified Mason-Allen technique. A 23-gauge needle was used to make 2 angled holes at either end of the supraspinatus footprint. The suture was then passed through the bone using the holes and tightened until the cut end of the tendon was secured back to its footprint.

In the intervention group, the collagen scaffold (5×2 mm) was rehydrated with sterile saline solution and then overlaid longitudinally on the superficial aspect of the tendon-bone insertion. It was then secured to the tendon via a mattress suture proximally and through a separate bone tunnel distally in the proximal humerus below the supraspinatus footprint (Fig. 1, *b*, shows positioning of the scaffold before placement of the distal sutures).

After repair, the coracoacromial arch and the deltoid were reapproximated with interrupted No. 4-0 Vicryl sutures. Skin closure was carried out with a running subcuticular No. 4-0 Monocryl suture (Ethicon) with buried knots at both ends. After closure, 0.4 mL of bupivacaine local anesthetic (1.25-mg/mL solution) was infiltrated around the incision.

Table I Histologic grading system for assessment of supraspinatus tendon healing

Grade	Collagen fiber density	Collagen fiber orientation	Bone-tendon interface	Vascularity	Inflammation
0	None	None	0%-24% interdigitation	Abundant vascular network	Abundant inflammatory cells
1	Low	Disorganized fibers	25%-49% interdigitation	Moderate vascular network	Moderate inflammatory cells
2	Medium	Moderate alignment	50%-75% interdigitation	Minimal vascular network	Minimal inflammatory cells
3	High	Highly aligned	>75% interdigitation	No vascular network	No inflammatory cells

The rats were closely monitored after surgery. Once they had sufficiently recovered from the anesthetic, they were housed singularly and transferred to a warming cabinet for 1 night. Carprofen (10 μL/g) and 2 mL of normal saline solution were administered subcutaneously twice daily for 48 hours postoperatively. The rats were weighed daily and checked for signs of illness, pain, or distress twice daily for the first 48 hours postoperatively. After this, they were weighed and checked once daily until 14 days postoperatively. They were then weighed and checked on a weekly basis.

At either 6 or 12 weeks postoperatively, the rats were humanely killed by carbon dioxide inhalation. The left shoulder was immediately excised. The entirety of the supraspinatus muscle and the humerus was then either placed in formalin for histologic analysis (20 samples, 10 at each time point) or wrapped in phosphate-buffered saline solution–soaked gauze and stored at −20°C for later biomechanical analysis (20 samples, 10 at each time point). In the 6 sham animals (3 at each time point), both shoulders were excised and one each was used for histologic analysis and biomechanical analysis.

Biomechanical analysis

The excised samples were defrosted at room temperature and kept hydrated with normal saline solution spray throughout testing. The supraspinatus muscle fibers were removed by scraping with a sharp scalpel, leaving only the distal tendon and its attachment to bone. Any residual suture material was also removed.

The humerus and the tendon were positioned in an Instron machine (Instron, Norwood, MA, USA) with a 1-kN load cell. The tendon was secured using a double screw clamp and fine-grit sandpaper, and the humerus was secured using a vice to prevent fracture through the growth plate.[13] Specimens underwent a 10-cycle preconditioning phase (0.1 to 0.5 N at a rate of 1%/s), followed by 10 minutes of relaxation, and were then stretched to failure at a rate of 0.3%/s. The stiffness, Young modulus, and ultimate load at failure were recorded for each sample. For each treatment group, 5 samples were tested at each time point (6 and 12 weeks).

Histologic analysis

Samples were fixed in 10% neutral buffered formalin for 7 days, followed by decalcification in 10% formic acid for 7 days. Finally, the samples were transferred to 70% ethanol and embedded in paraffin, and 7-μm sections were taken. Sections were stained with hematoxylin-eosin and viewed using both transmitted and polarized light. A semiquantitative grading system, previously described by our group, was used to grade healing (Table I).[33]

Scoring was carried out by an experienced musculoskeletal histopathologist and the lead author, both of whom were blinded to the treatment groups. A minimum of 3 slides per sample were assessed. For each treatment group, 5 specimens were assessed at each time point.

Statistical analysis

Data from both the in vitro and in vivo analyses were analyzed using the Mann-Whitney *U* test for continuous variables and the Fisher exact test for categorical variables (GraphPad, San Diego, CA, USA). $P < .05$ was considered significant.

Results

Qualitative and quantitative analyses of scaffold cytocompatibility

After cell culture and alamarBlue staining, quantitative analysis demonstrated increasing cell numbers from day 1 to day 7 of experimentation (Fig. 2). Specifically, fluorescence intensity, a linear measure of cell numbers, increased from 57.5% of control on day 1 to 83.8% on day 3 and 182.3% on day 7. The difference between the groups was statistically significant ($P = .0001$). Qualitative analysis using fluorescent microscopy with CellTracker Green CMFDA Dye demonstrated the successful adherence of primary tendon-derived cells to the scaffold on day 1. Over the 7-day period, the number of cells increased while maintaining their morphology (Fig. 3).

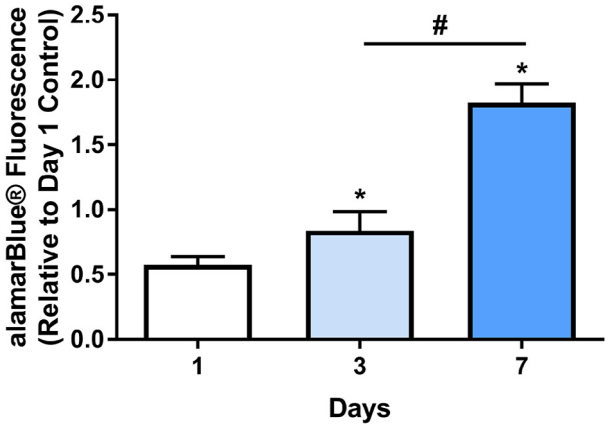

Figure 2 Primary human tendon-derived cell growth as assessed by alamarBlue increased on the scaffolds over a 7-day period. #Significant difference. *Statistically significant difference between the two labelled groups.

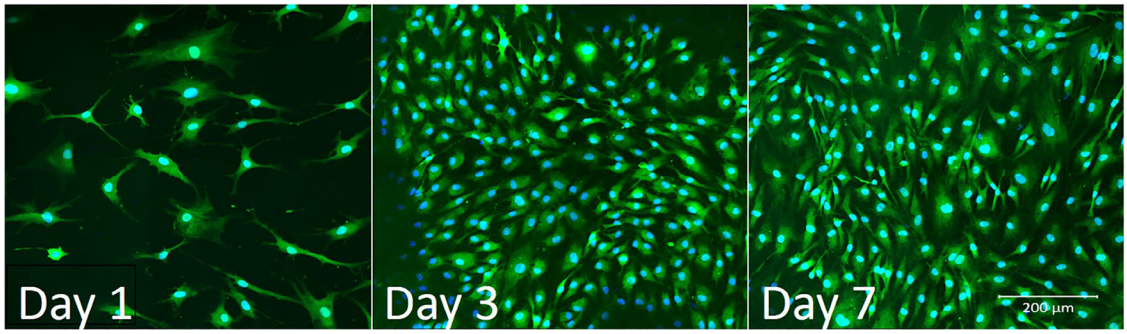

Figure 3 Primary human tendon-derived cells adhered to the scaffold and increased in number over a 7-day period; cell morphology was maintained (CellTracker Green CMFDA Dye, original magnification ×40).

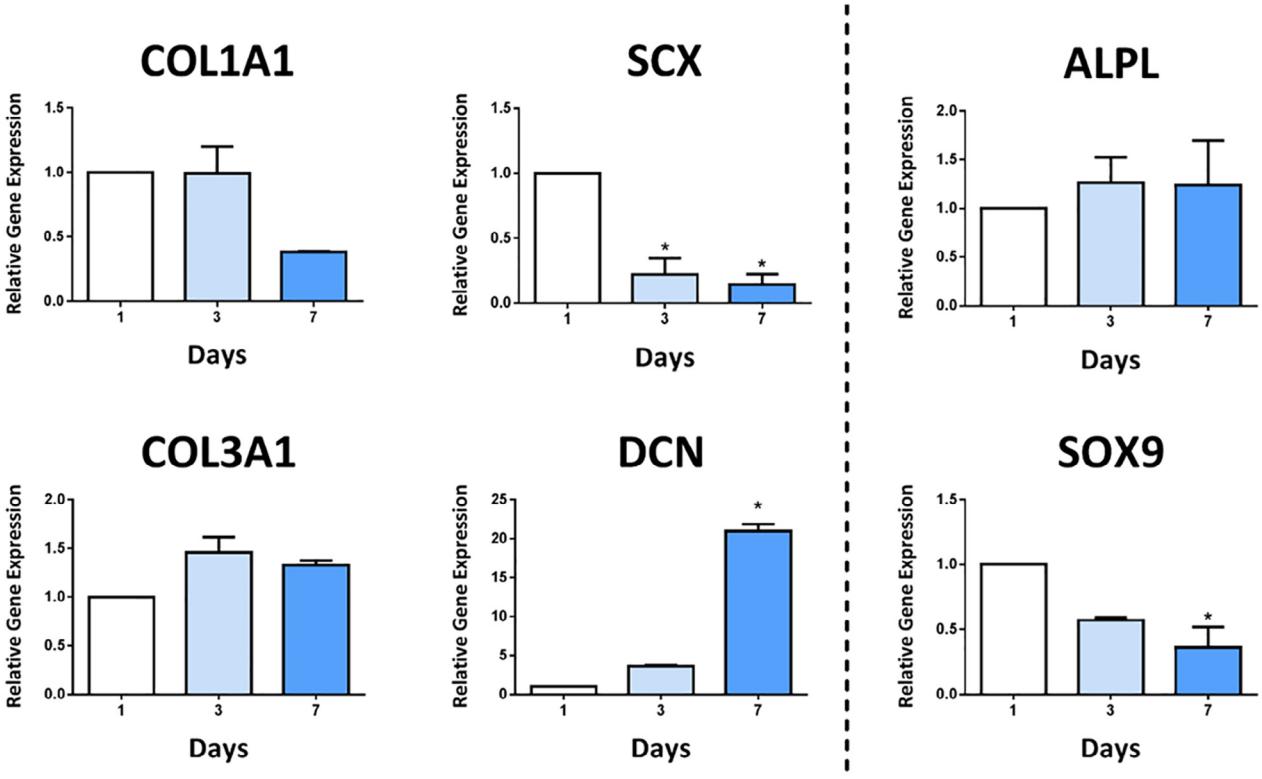

Figure 4 Cell gene expression when cultured on the scaffold over a 7-day period. *COL1A1*, collagen type I alpha 1 chain; *SCX*, scleraxis; *ALPL*, alkaline phosphatase; *COL3A1*, collagen type III alpha 1 chain; *DCN*, decorin. *Statistically significant difference between the two labelled groups.

Gene expression

The expression of 4 tendon-specific genes, 1 bone-specific gene, and 1 fibrocartilage-specific gene was assessed on days 1, 3, and 7 after cultivation of tendon-derived cells on scaffolds. Gene expression was expressed as a proportion of control (gene expression at the time of cell harvest). The relative gene expression of collagen type I alpha 1 chain (*COL1A1*) and collagen type III alpha 1 chain (*COL3A1*) was maintained up to day 3; however, we observed a decrease in the expression of scleraxis (*SCX*) over the experimental period. Decorin expression was increased over the experimental period. The expression of the bone-specific alkaline phosphatase (*ALPL*) gene was maintained over 7 days, whereas the cartilage-specific *SOX9* gene expression steadily decreased over the experimental period (Fig. 4).

Immunogenicity assay

After 24 and 48 hours of exposure to the collagen scaffold, human monocyte (THP-1) expression levels of interleukin 1β were comparable to controls, with an increase of 6% on day 1 and 32% on day 2. These differences were not statistically significant. Vicryl sutures caused a significant 82% increase in relative expression on day 1 and a 350% increase on day 2. The scaffold material also had no significant impact on

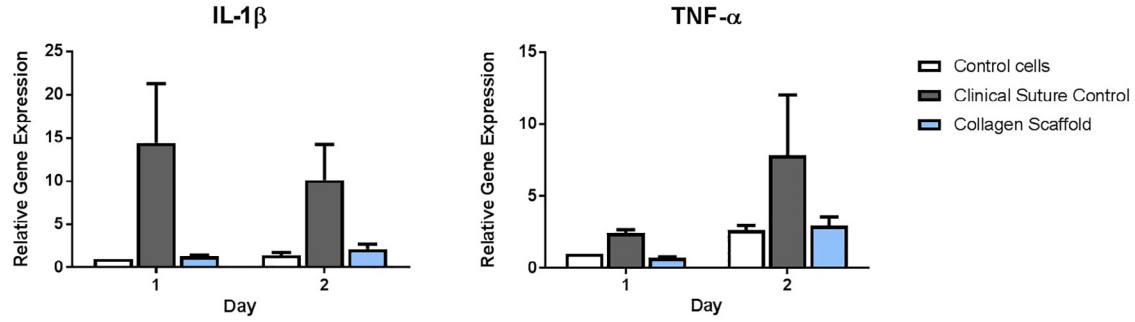

Figure 5 Proinflammatory gene expression was not significantly increased by the collagen scaffold material. *IL-1β*, interleukin 1β; *TNF-α*, tumor necrosis factor α.

tumor necrosis factor α expression, with a 15% decrease on day 1 and a 26% increase on day 2. Again, this contrasted with a 232% increase on day 1 and a 580% increase on day 2 caused by the Vicryl suture material (Fig. 5).

In vivo

All surgical procedures were successful with no intraoperative complications. All rats recovered well and were able to use the operated limb by 48 hours postoperatively. All 46 animals survived the experimental period. No wound infection or discharge was observed.

At the time of the cull, the scaffold was found to still be visible at 6 weeks but difficult to distinguish clearly at 12 weeks, suggesting bio-integration. Furthermore, macroscopic inspection of the collected specimens did not reveal any gross infectious or inflammatory changes.

Biomechanical analysis

Testing was successfully completed using the aforementioned setup in all samples; all failures occurred at the bone-tendon junction. At 6 weeks, the stiffness and Young modulus achieved in the scaffold group were lower than those in the control group. The average load at failure was 28.3 N in the scaffold group and 34.0 N in the control group. This difference was not statistically significant ($P = .42$). At 12 weeks, the mechanical performance of the scaffold group improved and outperformed the control group in stiffness, the Young modulus, and ultimate load at failure. However, the differences were not statistically significant (Fig. 6, Table II).

Histologic analysis

At 6 weeks postoperatively, the quality of healing was similar in both groups. In most samples, the tendon fibers were moderately disorganized. The bone-tendon junction appeared intact but did not exhibit a mature transitional zone. The average histologic score was 5.9 in the control group and 6.8 in the scaffold group ($P = .69$); both were lower than the score of 10.5 in the sham group (Figs. 7, 8).

Table II Biomechanical testing results

	Load at failure, N	Stiffness, N/mm	Young modulus, MPa
6 weeks			
Control	34.0	20.0	20.4
Scaffold	28.3	26.9	17.3
P value	.42	.31	.55
12 weeks			
Control	32.9	17.5	14.3
Scaffold	37.4	20.4	19.7
P value	.91	.56	.11

At 12 weeks postoperatively, the sham group exhibited normal collagen fiber alignment with a mature transition zone at the bone-tendon junction. Little improvement was observed in the control group; tendon fiber disorganization was still present, and the bone-tendon junction was predominantly made up of fibers inserting directly onto bone without the formation and maturation of a fibrocartilage transition zone. In the scaffold group, we observed improved collagen fiber density and orientation scores in the tendon. We also observed an improved enthesis with early formation of a fibrocartilage transition zone in 2 of 5 samples. No differences were observed in vascular formations and inflammatory changes between the groups. Overall, the scaffold group showed an average histologic score of 8.4 compared with 6.6 in the control group ($P = .032$). Again, scores from both groups were lower than the score in the sham group (Table III).

Discussion

In this study, we have demonstrated that a new synthetic collagen scaffold promoted cell growth without eliciting an acute immunologic response in vitro. With an in vivo rat rotator cuff model, the scaffold improved the quality of healing as assessed by histology at 12 weeks postoperatively.

Tissue scaffolds are commonly used adjuvants for rotator cuff repair.[16,27,33] A number of products, mostly derived from decellularized cadaveric or animal tissues, are available to the

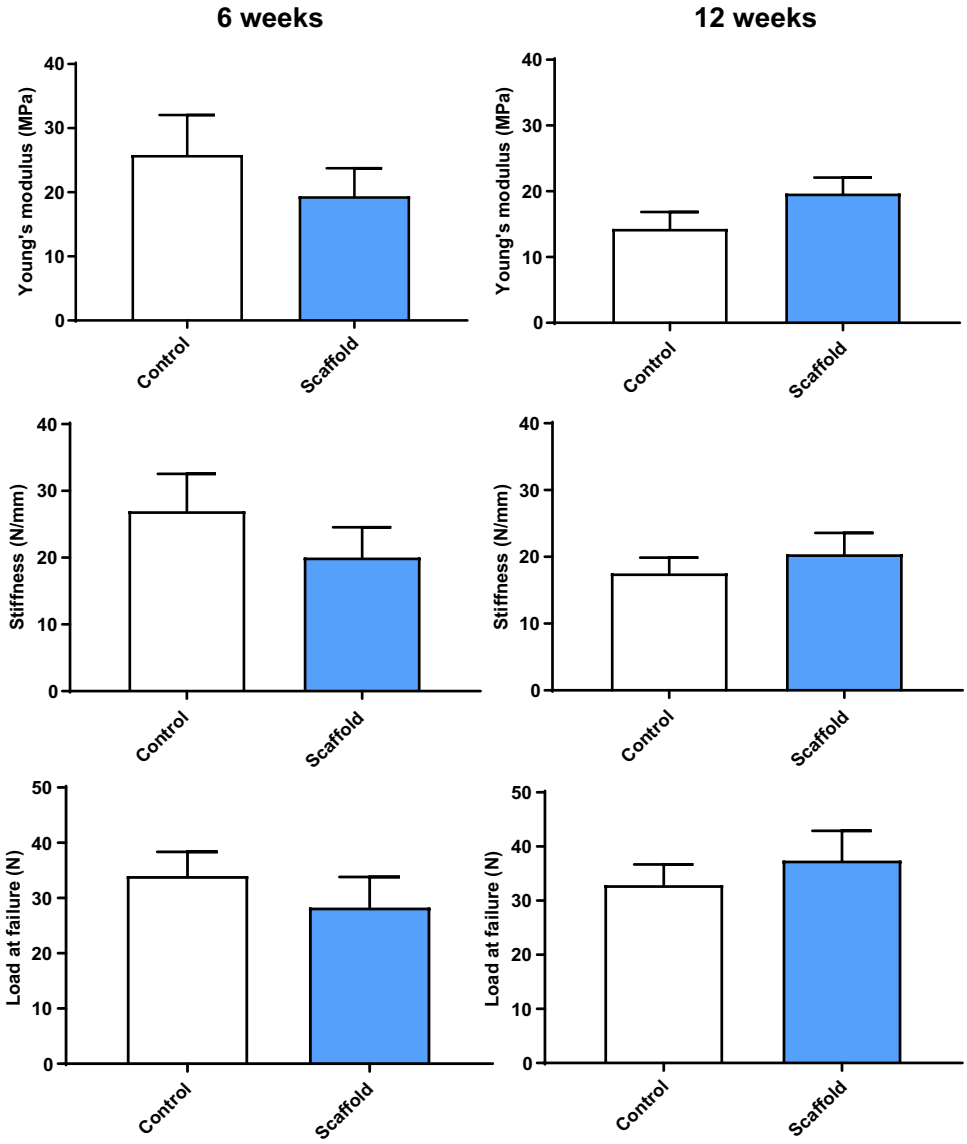

Figure 6 Biomechanical analysis shows a lower Young modulus, stiffness, and load at failure in the scaffold-treated group compared with the control group at 6 weeks. However, all 3 parameters increased in the scaffold group by 12 weeks, whereas the control group did not show improvement. No significant differences were found in any comparison.

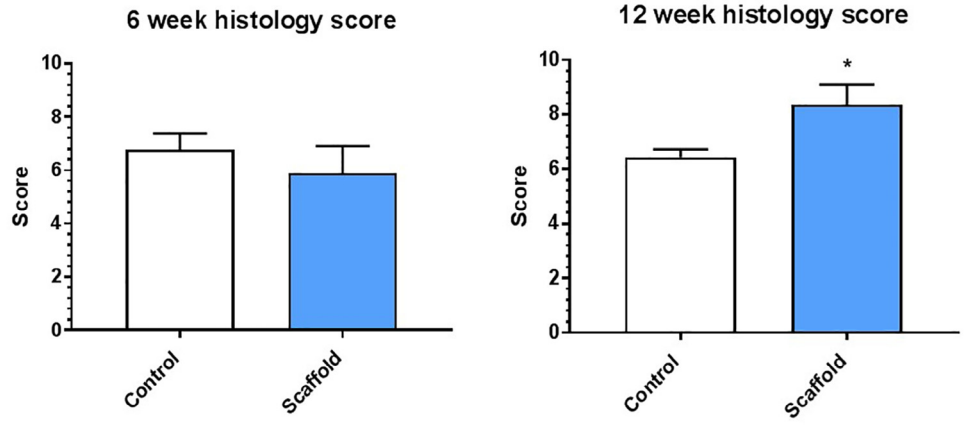

Figure 7 Histologic analysis showed no significant difference in the histologic score at 6 weeks but showed a significantly higher score in the scaffold group compared with the control group at 12 weeks (*).

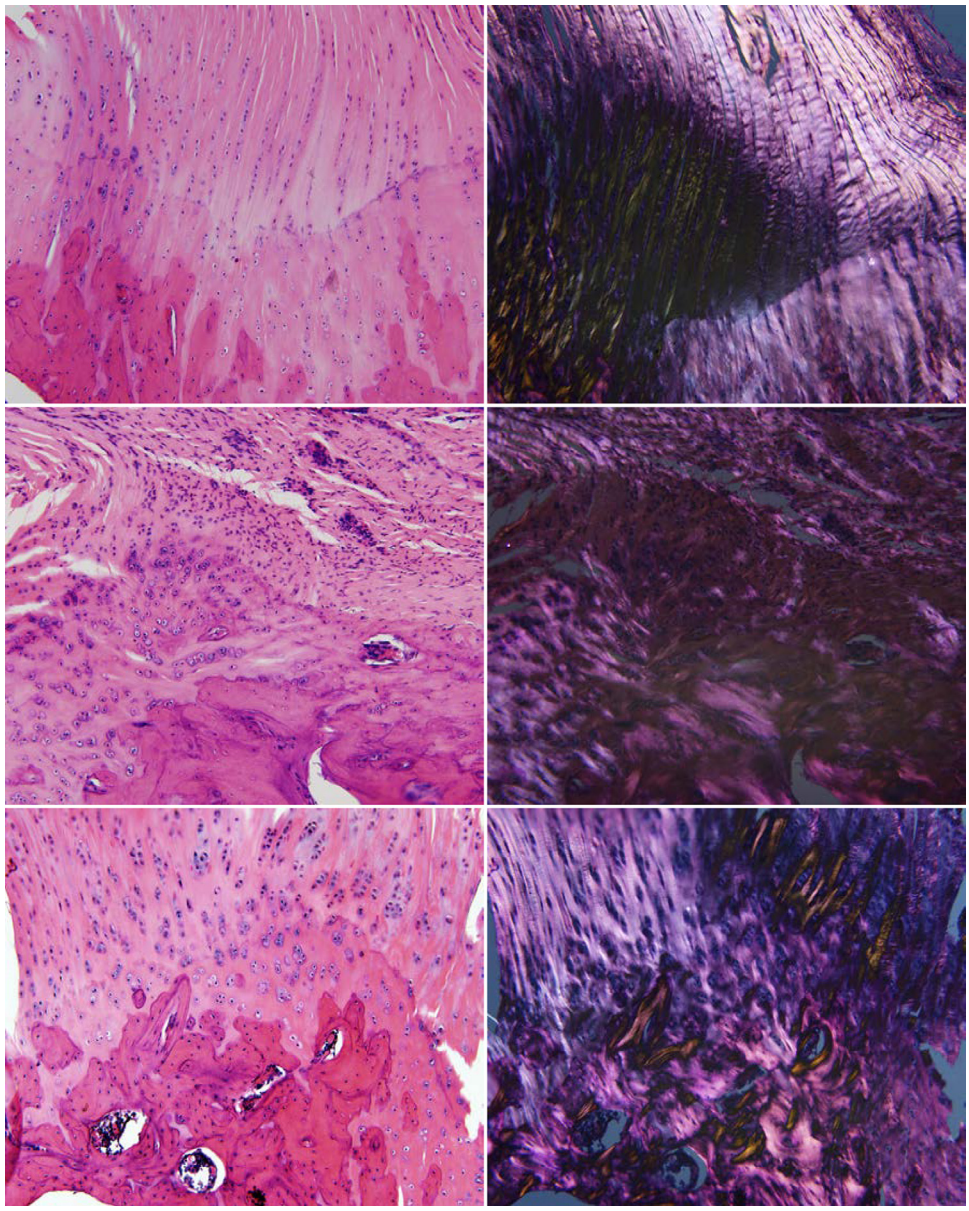

Figure 8 Transmitted light (*left*) and polarized light (*right*) images showing normal collagen fiber alignment and fibrocartilage bone-tendon junction in sham group (*top row*); emergence of fibrocartilage transition zone with disorganization of collagen fibers still evident after control repair (*middle row*); and maturing bone-tendon junction with good alignment of collagen fibers after scaffold repair (*bottom row*).

Table III Detailed histologic scores

	Density	Orientation	Bone-tendon interface	Vascularity	Inflammation	Total
6 weeks						
Sham	2.2 (0.4)	2.4 (0.3)	2.2 (0.2)	2.2 (0.2)	1.5 (0.2)	10.5 (1.2)
Control	1.5 (0.1)	1.4 (0.2)	1.2 (0.1)	1.6 (0.3)	0.9 (0.1)	6.8 (0.6)
Scaffold	1.6 (0.2)	1.1 (0.3)	1.2 (0.4)	1.4 (0.4)	0.7 (0.2)	5.9 (1.0)
12 weeks						
Sham	2.3 (0.4)	2.4 (0.4)	2.7 (0.3)	2.3 (0.3)	2.3 (0.4)	11.9 (1.1)
Control	1.4 (0.2)	1.2 (0.2)	1.2 (0.2)	1.5 (0.1)	1.1 (0.1)	6.6 (0.4)
Scaffold	1.9 (0.1)	1.7 (0.3)	2.0 (0.3)	1.3 (0.2)	1.5 (0.2)	8.4 (0.7)

Data are reported as mean (standard error).

orthopedic surgeon.[2,32] These tissue scaffolds have several significant drawbacks preventing their uptake; these include potential immune reactions, uncertainties regarding long-term bio-integration, and prohibitive costs.[2,8,30] The new collagen scaffold used in this study is free of cellular debris and DNA material.[38] Furthermore, the manufacturing process ensures that layers of collagen are laid down along the long axis of the scaffold, providing an ordered matrix for the infiltration and growth of cells.[38]

In vitro assessment clearly demonstrated that tendon-derived cells were able to successfully survive on the scaffold over a 7-day period. Furthermore, qualitative analysis revealed preservation of cell shape, an important feature of tenocyte health.[20] The scaffold exhibited minimal acute immunogenicity, lower than that of commonly used suture material. These properties of the scaffold in vitro allowed us to proceed to the in vivo phase of the study.

As healing occurs, it is hoped that the collagen scaffold can be incorporated into the native tendon tissue and improve the quality of healing and therefore strength at the bone-tendon interface. This is a key requirement of successful scaffolds.[2,3,35] The new collagen scaffold used in this study remained clearly visible at 6 weeks. At 12 weeks, the scaffolds were incorporated into the surrounding tissue and were not clearly distinguishable. The scaffold group achieved a significantly improved histologic score compared with the control group at 12 weeks. This finding suggests that the incorporation of the scaffold at 12 weeks was associated with a meaningful increase in the quality of healing. It is important to note that there was no difference in inflammatory and vascular scores between the control and scaffold groups (Table II).

Although we did not observe improved mechanical performance in the scaffold group at 6 weeks postoperatively, the ultimate load at failure improved from 28.3 to 37.4 N by the 12-week time point. Again, this may be due to the incorporation of the scaffold seen at 12 weeks. In contrast, no improvements between the 2 time points were observed in the control group. Although we observed an improved histologic appearance of the scaffold group at 12 weeks, we did not observe a statistically significant difference in tendon mechanical properties between the groups. It must be noted that the weak point of the tested tendon-bone unit is at the tendon-bone junction where the repair took place. Therefore, the histologic score may not directly correlate with mechanical testing results, as bone-tendon junction assessment makes up only 1 category in histologic scoring.

This study has several limitations. First, because of the use of 2 time points, a limited number of animals (10 in each group) were available for histologic and biomechanical assessment at each time point. Second, the rat rotator cuff model has inherent limitations owing to its small size. Hence, repair methods such as bone anchors and double-row suturing cannot be easily adapted to the rat model. Last, the acute detachment used in this model may not reflect the chronic, degenerative nature of rotator cuff tears in patients. Before clinical use, assessment using a chronic, large animal model is necessary.

Conclusion

This study demonstrated that a new collagen scaffold was supportive of tendon-derived cell growth and not acutely immunogenic in vitro. In a rat model of rotator cuff tears, overlying supraspinatus tendon repair with the scaffold improved the quality of healing at the tendon and the bone-tendon junction. Further refinement and testing of the scaffold are required prior to consideration for clinical use.

Acknowledgment

We acknowledge the contribution of Dr. Satya Amirapu for her assistance with histologic evaluation and Professor Ashvin Thambyah for his assistance with biomechanical testing.

Disclaimer

The study was funded by the University of Auckland through a Uniservices grant (grant No. 32312.002).

Nicola Dalbeth reports research grant funding from Amgen and AstraZeneca; speaker fees from Pfizer, Horizon, Janssen, and Abbvie; and consulting fees from Horizon and Kowa, outside the submitted work. All the other authors, their immediate families, and any research foundations with which they are affiliated have not received any financial payments or other benefits from any commercial entity related to the subject of this article.

References

1. Abtahi AM, Granger EK, Tashjian RZ. Factors affecting healing after arthroscopic rotator cuff repair. World J Orthop 2015;6:211-20. http://dx.doi.org/10.5312/wjo.v6.i2.211
2. Amini MH, Ricchetti ET, Iannotti JP, Derwin KA. An update on scaffold devices for rotator cuff repair. Tech Shoulder Elbow Surg 2017;18:101-12. http://dx.doi.org/10.1097/BTE.0000000000000122
3. Arnoczky SP, Bishai SK, Schofield B, Sigman S, Bushnell BD, Hommen JP, et al. Histologic evaluation of biopsy specimens obtained after rotator cuff repair augmented with a highly porous collagen implant arthroscopy. Arthroscopy 2017;33:278-83. http://dx.doi.org/10.1016/j.arthro.2016.06.047
4. Barber FA, Burns JP, Deutsch A, Labbé MR, Litchfield RB. A prospective, randomized evaluation of acellular human dermal matrix augmentation for arthroscopic rotator cuff repair. Arthroscopy 2012;28:8-15. http://dx.doi.org/10.1016/j.arthro.2011.06.038
5. Baring TKA, Cashman PPM, Reilly P, Emery RJH, Amis AA. Rotator cuff repair failure in vivo: a radiostereometric measurement study. J Shoulder Elbow Surg 2011;20:1194-9. http://dx.doi.org/10.1016/j.jse.2011.04.010

6. Boileau P, Brassart N, Watkinson DJ, Carles M, Hatzidakis AM, Krishnan SG. Arthroscopic repair of full-thickness tears of the supraspinatus: does the tendon really heal? J Bone Joint Surg 2005;87:1229-40. http://dx.doi.org/10.2106/JBJS.D.02035
7. Bryant D, Holtby R, Willits K, Litchfield R, Drosdowech D, Spouge A, et al. A randomized clinical trial to compare the effectiveness of rotator cuff repair with or without augmentation using porcine small intestine submucosa for patients with moderate to large rotator cuff tears: a pilot study. J Shoulder Elbow Surg 2016;25:1623-33. http://dx.doi.org/10.1016/j.jse.2016.06.006
8. Cheung E, Silverio L, Sperling J. Strategies in biologic augmentation of rotator cuff repair: a review. Clin Orthop Relat Res 2010;468:1476-84. http://dx.doi.org/10.1007/s11999-010-1323-7
9. Chhana A, Callon KE, Dray M, Pool B, Naot D, Gamble GD, et al. Interactions between tenocytes and monosodium urate monohydrate crystals: implications for tendon involvement in gout. Ann Rheum Dis 2014;73:1737-41. http://dx.doi.org/10.1136/annrheumdis-2013-204657
10. Cho NS, Yi JW, Lee BG, Rhee YG. Retear patterns after arthroscopic rotator cuff repair: single-row versus suture bridge technique. Am J Sports Med 2010;38:664-71. http://dx.doi.org/10.1177/0363546509350081
11. Coghlan JA, Buchbinder R, Green S, Johnston RV, Bell SN. Surgery for rotator cuff disease. Cochrane Database Syst Rev 2008;(1):CD005619. http://dx.doi.org/10.1002/14651858.CD005619.pub2
12. Daly KA, Stewart-Akers AM, Hara H, Ezzelarab M, Long C, Cordero K, et al. Effect of the αGal epitope on the response to small intestinal submucosa extracellular matrix in a nonhuman primate model. Tissue Eng Part A 2009;15:3877-88. http://dx.doi.org/10.1089/ten.tea.2009.0089
13. Deren ME, Ehteshami JR, Dines JS, Drakos MC, Behrens SB, Doty S, et al. Simvastatin exposure and rotator cuff repair in a rat model. Orthopedics 2017;40:e288-92. http://dx.doi.org/10.3928/01477447-20161128-02
14. Docheva D, Müller SA, Majewski M, Evans CH. Biologics for tendon repair. Adv Drug Deliv Rev 2015;84(Suppl C):222-39. http://dx.doi.org/10.1016/j.addr.2014.11.015
15. Gilbert TW, Freund JM, Badylak SF. Quantification of DNA in biologic scaffold materials. J Surg Res 2009;152:135-9. http://dx.doi.org/10.1016/j.jss.2008.02.013
16. Hakimi O, Mouthuy P, Carr A. Synthetic and degradable patches: an emerging solution for rotator cuff repair. Int J Exp Pathol 2013;94:287-92. http://dx.doi.org/10.1111/iep.12030
17. Iannotti JP, Codsi MJ, Kwon YW, Derwin K, Ciccone J, Brems JJ. Porcine small intestine submucosa augmentation of surgical repair of chronic two-tendon rotator cuff tears. A randomized, controlled trial. J Bone Joint Surg Am 2006;88:1238-44. http://dx.doi.org/10.2106/JBJS.E.00524
18. Iannotti JP, Deutsch A, Green A, Rudicel S, Christensen J, Marraffino S, et al. Time to failure after rotator cuff repair: a prospective imaging study. J Bone Joint Surg 2013;95:965-71. http://dx.doi.org/10.2106/JBJS.L.00708
19. Judge A, Murphy RJ, Maxwell R, Arden NK, Carr AJ. Temporal trends and geographical variation in the use of subacromial decompression and rotator cuff repair of the shoulder in England. Bone Joint J 2014;96B:70-4. http://dx.doi.org/10.1302/0301-620X.96B1.32556
20. Longo UG, Franceschi F, Ruzzini L, Rabitti C, Morini S, Maffulli N, et al. Histopathology of the supraspinatus tendon in rotator cuff tears. Am J Sports Med 2008;36:533-8. http://dx.doi.org/10.1177/0363546507308549
21. Ma CB. Editorial commentary: success of rotator cuff healing-do we need to improve on the strength anymore? Arthroscopy 2017;33:1659-60. http://dx.doi.org/10.1016/j.arthro.2017.06.017
22. Mather RC III, Richard C, Koenig L, Acevedo D, Dall TM, Gallo P, et al. The societal and economic value of rotator cuff repair. J Bone Joint Surg Am 2013;95:1993-2000. http://dx.doi.org/10.2106/JBJS.L.01495
23. McElvany MD, McGoldrick E, Gee AO, Neradilek MB, Matsen FA III. Rotator cuff repair: published evidence on factors associated with repair integrity and clinical outcome. Am J Sports Med 2015;43:491-500. http://dx.doi.org/10.1177/0363546514529644
24. Miller BS, Downie BK, Kohen RB, Kijek T, Lesniak B, Jacobson JA, et al. When do rotator cuff repairs fail? Serial ultrasound examination after arthroscopic repair of large and massive rotator cuff tears. Am J Sports Med 2011;39:2064-70. http://dx.doi.org/10.1177/0363546511413372
25. Patel S, Gualtieri AP, Lu HH, Levine WN. Advances in biologic augmentation for rotator cuff repair. Ann N Y Acad Sci 2016;1383:97-114. http://dx.doi.org/10.1111/nyas.13267
26. Ricchetti E, Aurora A, Iannotti J, Derwin E. Scaffold devices for rotator cuff repair. J Shoulder Elbow Surg 2012;21:251-65. http://dx.doi.org/10.1016/j.jse.2011.10.003
27. Richter DL, Brockmeier SF. Arthroscopic patch augmentation for rotator cuff repair. Tech Shoulder Elbow Surg 2016;17:144-8. http://dx.doi.org/10.1097/BTE.0000000000000112
28. Rodeo SA, Potter HG, Kawamura S, Turner AS, Kim HJ, Atkinson BL. Biologic augmentation of rotator cuff tendon-healing with use of a mixture of osteoinductive growth factors. J Bone Joint Surg 2007;89:2485-97. http://dx.doi.org/10.2106/JBJS.C.01627
29. Rothrauff BB, Pauyo T, Debski RE, Rodosky MW, Tuan RS, Musahl V. The rotator cuff organ: integrating developmental biology, tissue engineering, and surgical considerations to treat chronic massive rotator cuff tears. Tissue Eng Part B Rev 2017;23:318-35. http://dx.doi.org/10.1089/ten.teb.2016.0446
30. Ryu RKN. Editorial commentary: outcomes after patch use in rotator cuff surgery: searching for the "holy grail". Arthroscopy 2016;32:1691-2. http://dx.doi.org/10.1016/j.arthro.2016.05.027
31. Savin D, Meadows M, Verma N, Cole B. Rotator cuff healing: improving biology. Oper Tech Sports Med 2017;25:34-40. http://dx.doi.org/10.1053/j.otsm.2016.12.006
32. Smith RDJ, Zargar N, Brown CP, Nagra NS, Dakin SG, Snelling SJB, et al. Characterizing the macro and micro mechanical properties of scaffolds for rotator cuff repair. J Shoulder Elbow Surg 2017;26:2038-46. http://dx.doi.org/10.1016/j.jse.2017.06.035
33. Street M, Thambyah A, Dray M, Amirapu S, Tuari D, Callon KE, et al. Augmentation with an ovine forestomach matrix scaffold improves histological outcomes of rotator cuff repair in a rat model. J Orthop Surg 2015;10:165. http://dx.doi.org/10.1186/s13018-015-0303-8
34. Thangarajah T, Pendegrass CJ, Shahbazi S, Lambert S, Alexander S, Blunn GW. Augmentation of rotator cuff repair with soft tissue scaffolds orthopaedic. J Sports Med 2015;3:2325967115587495. http://dx.doi.org/10.1177/2325967115587495
35. Van Kampen C, Arnoczky S, Parks P, Hackett E, Ruehlman D, Turner A, et al. Tissue-engineered augmentation of a rotator cuff tendon using a reconstituted collagen scaffold: a histological evaluation in sheep. Muscles Ligaments Tendons J 2013;3:229.
36. Wildemann B, Klatte F. Biological aspects of rotator cuff healing. Muscles Ligaments Tendons J 2011;1:161.
37. Yamaguchi K, Ditsios K, Middleton WD, Hildebolt CF, Galatz LM, Teefey SA. The demographic and morphological features of rotator cuff disease. A comparison of asymptomatic and symptomatic shoulders. J Bone Joint Surg Am 2006;88:1699-704. http://dx.doi.org/10.2106/JBJS.E.00835
38. Zhang J, Sisley AMG, Anderson AJ, Taberner AJ, McGhee CNJ, Patel DV. Characterization of a novel collagen scaffold for corneal tissue engineering. Tissue Eng Part C Methods 2015;22:165-72. http://dx.doi.org/10.1089/ten.tec.2015.0304
39. Zheng MH, Chen J, Kirilak Y, Willers C, Xu J, Wood D. Porcine small intestine submucosa (SIS) is not an acellular collagenous matrix and contains porcine DNA: possible implications in human implantation. J Biomed Mater Res B Appl Biomater 2005;73:61-7. http://dx.doi.org/10.1002/jbm.b.30170
40. Zumstein M, Lädermann A, Raniga S, Schär M. The biology of rotator cuff healing. Orthop Traumatol Surg Res 2017;103(Suppl):S1-10. http://dx.doi.org/10.1016/j.otsr.2016.11.003